

The evolution and persistence of dumbbells in electroweak theory

Jon Urrestilla^{1,2}, Ana Achúcarro^{1,3}, Julian Borrill^{4,5} and Andrew R. Liddle²

¹*Department of Theoretical Physics, UPV-EHU, Bilbao, Spain*

²*Astronomy Centre, University of Sussex, Falmer, Brighton BN1 9QJ, United Kingdom*

³*Institute for Theoretical Physics, University of Groningen, The Netherlands*

⁴*Center for Particle Astrophysics, University of California, Berkeley, CA 94720*

⁵*National Energy Research Scientific Computing Center, Lawrence Berkeley National Laboratory, University of California, Berkeley, CA 94720*

(May 20, 2019)

We use large-scale numerical simulations to study the formation and evolution of non-topological defects in an electroweak phase transition described by the Glashow–Salam–Weinberg model without fermions. Such defects include dumbbells, comprising a pair of monopoles joined by a segment of electroweak string. These exhibit complex dynamics, with some shrinking under the string tension and others growing due to the monopole–antimonopole attractions between near neighbours. We estimate the range of parameters where the network of dumbbells persists, and show that this region is narrower than the region within which infinite straight electroweak strings are perturbatively stable.

Preprint hep-ph/0106282

I. INTRODUCTION

As the early Universe expanded and cooled, it is very likely that it underwent a number of symmetry-breaking phase transitions during which topological and non-topological defects could have formed via the Kibble mechanism [1,2]. A number of symmetry breaking schemes have been proposed in particle physics with different degrees of success. In particular it is almost certain that some sort of transition occurs at the electroweak scale, and therefore it is important to understand what defects, if any, could form during that symmetry breaking.

The formation of topological defects in any phase transition depends on the existence of a non-trivial, low-order homotopy group of the broken-symmetry vacuum manifold [1,2]. Even in the absence of this, dynamically stable non-topological defects are sometimes still possible, but are usually assumed to be too weakly stable to lead to a lasting network. A particularly interesting case is non-topological strings where at least one example is known (semilocal strings [3,4]) in which a space-spanning network of strings can develop from the growth and joining of short string segments formed at the phase transition [5]. Semilocal strings are a special case of electroweak strings [6–8] and in this paper we will investigate if other types of electroweak string could also lead to persistent networks.

The stability of electroweak strings has been analyzed in some detail in the Glashow–Salam–Weinberg (GSW) model in the absence of fermions; in that case the theory is determined, up to scalings, by only two parameters: the weak mixing angle θ_W , and β which is the square of the ratio of the Higgs and Z -boson masses. In this paper we will consider phase transitions in the generalized class of GSW models in which the weak mixing angle and β may take on any values (note that the observed value for the actual electroweak model is $\sin^2\theta_W = 0.23$, and the precise value of β has not yet been determined but is almost certainly greater than one).

In the case of interest here, the topology of the vacuum manifold is the three-sphere S^3 , which does not support persistent topological defects in 3+1 dimensional spacetime, but there are grounds for expecting non-topological defects to form. In the limit $\theta_W = \pi/2$ we recover the so-called semilocal model, whose S^3 vacuum manifold is known to support stable non-topological strings from both analytical [3,4] and numerical [5] work. In particular, a straight infinite semilocal string can be seen as a Nielsen–Olesen (NO) $U(1)$ vortex [9], embedded in a higher group $SU(2)_{\text{global}} \times U(1)_{\text{local}}$.

The embedding of NO vortices into the full electroweak symmetry $SU(2)_L \times U(1)_Y$ leads to Z -strings and W strings (see [8]). Although W -strings are expected to be unstable, analysis of infinite axially-symmetric Z -strings has shown the existence of a parameter regime where they are perturbatively stable [10]. Nambu [6] also proposed a configuration consisting of monopole–antimonopole pairs joined by Z -string segments, and named these objects *dumbbells*. Isolated dumbbells are expected to collapse under the string tension, but Nambu suggested that their lifetime could be increased by rotation (for physical values of the parameters in the GSW model the expected dumbbell masses are in the region of a few TeV, and their lifetime may be long enough for detection in particle accelerators). When the density of dumbbells is sufficiently high, another possibility is the linking of string segments due to the interaction of neighbouring monopoles.

In this paper we study the formation of electroweak string networks using numerical methods. Isolated, infinite, axially-symmetric Z -string configurations will not be formed in a realistic system, but dumbbells are certainly possible. Of particular interest, therefore, is the question of whether there is a region of parameter space in which these are able to generate a persistent network of strings by building up longer segments from the merging of shorter ones, as has been found in the semilocal case [5].

II. THE MODEL

The bosonic sector of the GSW electroweak model describes an $SU(2)_L \times U(1)_Y$ invariant theory with a scalar field Φ in the fundamental representation of $SU(2)_L$, with Lagrangian

$$\mathcal{L} = |D_\mu \Phi|^2 - \frac{1}{4} W_{\mu\nu}^a W^{a\mu\nu} - \frac{1}{4} Y_{\mu\nu} Y^{\mu\nu} + \lambda \left(\Phi \Phi^\dagger - \frac{\eta^2}{2} \right)^2. \quad (1)$$

The covariant derivative is given by

$$D_\mu \equiv \partial_\mu - \frac{ig_w}{2} \tau^a W_\mu^a - \frac{ig_y}{2} Y_\mu, \quad a = 1, 2, 3, \quad (2)$$

where Φ is a complex doublet, τ^a are the Pauli matrices, W_μ^a is a $SU(2)$ gauge field and Y_μ is a $U(1)$ gauge field. The field strengths associated with these gauge fields are

$$\begin{aligned} W_{\mu\nu}^a &= \partial_\mu W_\nu^a - \partial_\nu W_\mu^a + g_w \epsilon^{abc} W_\mu^b W_\nu^c; \\ Y_{\mu\nu} &= \partial_\mu Y_\nu - \partial_\nu Y_\mu, \end{aligned} \quad (3)$$

respectively, and there is no distinction between upper and lower group indices ($\epsilon^{123} = 1$).

When the scalar field acquires a non-zero vacuum expectation value the symmetry breaks from $SU(2)_L \times U(1)_Y$ to $U(1)_{\text{e.m.}}$, leaving a massive scalar field ($m_H = \sqrt{2\lambda}\eta$), a massless neutral photon (A_μ), a massive neutral Z -boson (Z_μ , $m_z = g_z\eta/2 \equiv l_v^{-1}$), and two massive charged W -bosons (W_μ^\pm , $m_W = g_w\eta/2$).

We make the following rescaling

$$\Phi \rightarrow \frac{\eta}{\sqrt{2}} \Phi, \quad x_\mu \rightarrow \frac{\sqrt{2}}{g_z \eta} x_\mu, \quad g_y Y_\mu \rightarrow \frac{g_z \eta}{\sqrt{2}} Y_\mu, \quad g_w W_\mu^a \rightarrow \frac{g_z \eta}{\sqrt{2}} W_\mu^a, \quad (4)$$

where $g_z = \sqrt{g_y^2 + g_w^2}$, to choose l_v as the unit of length, η as the unit of energy, and the Z -charge of the scalar field (g_z) as the unit of charge (up to numerical factors). This brings the classical field equations to the form

$$\begin{aligned} D^\mu D_\mu \Phi + \frac{2\lambda}{g_z^2} (\Phi \Phi^\dagger - 1) \Phi &= 0; \\ \partial_\nu W^{\mu\nu a} + \epsilon^{abc} W_\nu^b W^{\mu\nu c} &= \frac{i}{2} \cos^2 \theta_W \left[\Phi^\dagger \tau^a D^\mu \Phi - (D^\mu \Phi)^\dagger \tau^a \Phi \right]; \\ \partial_\nu Y^{\mu\nu} &= \frac{i}{2} \sin^2 \theta_W \left[\Phi^\dagger D^\mu \Phi - (D^\mu \Phi)^\dagger \Phi \right], \end{aligned} \quad (5)$$

where the weak mixing angle is given by $\tan \theta_W \equiv g_y/g_z$, and now

$$\begin{aligned} W_{\mu\nu}^a &\equiv \partial_\mu W_\nu^a - \partial_\nu W_\mu^a + \epsilon^{abc} W_\mu^b W_\nu^c; \\ D_\mu &\equiv \partial_\mu - \frac{i}{2} \tau^a W_\mu^a - \frac{i}{2} Y_\mu. \end{aligned} \quad (6)$$

Typically the Z - and A -fields are expressed in the unitary gauge $\Phi^T = (0, 1)$, but this choice is not well suited to work with defects. Instead, when there are points in space-time with $|\Phi| \neq 1$, it is customary to use a more general definition of these fields which depends on the Higgs field configuration at each point [6], namely,

$$\begin{aligned} Z_\mu &\equiv \cos \theta_W n^a(x) W_\mu^a - \sin \theta_W Y_\mu; \\ A_\mu &\equiv \sin \theta_W n^a(x) W_\mu^a + \cos \theta_W Y_\mu, \end{aligned} \quad (7)$$

where

$$n^a(x) \equiv -\frac{\Phi^\dagger(x)\tau^a\Phi(x)}{\Phi^\dagger(x)\Phi(x)}, \quad (8)$$

is a unit vector by virtue of the Fierz identity $\sum_a (\Phi^\dagger \tau^a \Phi)^2 = (\Phi^\dagger \Phi)^2$. There are also several possible definitions for the field strengths (see, e.g. Ref. [11]); in our simulations we will use

$$\begin{aligned} Z_{\mu\nu} &= \cos\theta_W n^a(x) W_{\mu\nu}^a - \sin\theta_W Y_{\mu\nu}; \\ A_{\mu\nu} &= \sin\theta_W n^a(x) W_{\mu\nu}^a + \cos\theta_W Y_{\mu\nu}. \end{aligned} \quad (9)$$

Note that equations (7) to (9) reduce to the usual definitions away from the defect cores. We work in flat space and in the temporal gauge ($W_0^a = Y_0 = 0$ for $a = 1, 2, 3$) so $D_0\Phi = \partial_0\Phi$. With this gauge choice, Gauss' Law becomes

$$\begin{aligned} -\partial_j(\partial_0 Y_j) &= \frac{i}{2} \sin^2\theta_W [\Phi^\dagger \partial_0 \Phi - (\partial_0 \Phi)^\dagger \Phi]; \\ -\partial_j(\partial_0 W_j^a) - \epsilon^{abc} W_j^b \partial_0 W_j^c &= \frac{i}{2} \cos^2\theta_W [\Phi^\dagger \tau^a \partial_0 \Phi - (\partial_0 \Phi)^\dagger \tau^a \Phi], \end{aligned} \quad (10)$$

(with $j = 1, 2, 3$) which is then used to test the stability of the code.

As noted above, the $\sin^2\theta_W = 1$ case reduces to the semilocal case, where absolutely stable defects are known to exist. Setting one of the Higgs fields to zero further reduces this to the abelian Higgs model. We are able to use our knowledge of these systems, as well as the behaviour of artificially constructed infinite axially-symmetric Z -strings at various points in parameter space, to check the validity of our simulation code.

III. NUMERICAL SIMULATIONS

The equations of motion (5) are discretized using a staggered leapfrog method. The simulations are then performed on a periodic cubic lattice whose time step is 0.2 times the spatial step $\Delta t = 0.2\Delta x$ ($c = 1$), with *ad hoc* numerical viscosity terms added to each equation ($\gamma \dot{\Phi}$, $\gamma \dot{Y}$ and $\gamma \dot{W}^a$ respectively) to reduce the system's relaxation time. The expansion rate in an expanding universe would play this role, albeit as a time-dependent factor $\gamma(t)$ typically scaling as $1/t$. Several different values of γ were tested, and generated very similar behaviour; throughout this work we use $\gamma = 0.5$.

Two different strategies for setting the initial configurations were considered:

a/ Set all initial field velocities to zero and throw down random scalar field phases at every lattice point; average the field at each point with its 6 nearest neighbours and normalize the fields to the vacuum value ($|\Phi|^2 = 1$ as η has been rescaled out) iteratively (50 times), to get a smoother configuration; using these scalar field values, choose the initial values of the gauge fields to be

$$\begin{aligned} Y_j(x) &= \frac{1}{2} \sin^2\theta_W (\psi_1 \nabla_j \psi_2 - \psi_2 \nabla_j \psi_1 + \psi_3 \nabla_j \psi_4 - \psi_4 \nabla_j \psi_3) \\ W_j^1(x) &= \frac{1}{2} \cos^2\theta_W (\psi_1 \nabla_j \psi_4 - \psi_4 \nabla_j \psi_1 + \psi_3 \nabla_j \psi_2 - \psi_2 \nabla_j \psi_3) \\ W_j^2(x) &= \frac{1}{2} \cos^2\theta_W (\psi_3 \nabla_j \psi_1 - \psi_1 \nabla_j \psi_3 + \psi_4 \nabla_j \psi_2 - \psi_2 \nabla_j \psi_4) \\ W_j^3(x) &= \frac{1}{2} \cos^2\theta_W (\psi_1 \nabla_j \psi_2 - \psi_2 \nabla_j \psi_1 + \psi_4 \nabla_j \psi_3 - \psi_3 \nabla_j \psi_4) \end{aligned} \quad (11)$$

where $\Phi^T = (\psi_1 + i\psi_2, \psi_3 + i\psi_4)$, pseudo-minimizing the energy as in Ref. [12].

b/ Set all fields to zero, and also gauge field velocities to zero ($\Phi = W_\mu^a = \dot{W}_\mu^a = Y_\mu = \dot{Y}_\mu = 0$); provide some initial (smoothed) random velocities to the scalar field ($\dot{\Phi} \neq 0$) following the general procedure as above.

The overall results in our simulations did not show qualitatively different behaviour between the two cases. Indeed, in the first case the gauge field energy pseudo-minimization was ineffective enough that the scalar field typically began by climbing up the potential, restoring the symmetric phase, and rolled down again later. For this reason, we chose the second initial configuration (b) for our investigations.

Interpreting simulations of electroweak string networks is more complicated than in the $U(1)$ cosmic string case. As in the semilocal case, electroweak strings are non-topological, and in this case there is no well-defined winding number, which makes identification of strings a more difficult task. We follow the strategy proposed in Ref. [12] in order to study string formation: the system is evolved forward in time and we compute a set of gauge-invariant quantities at each time step, namely the Z - and the A -field strengths given by Eq. (9) and the modulus of the scalar field ($|\Phi|$).

String formation is then observed by visualizing isosurfaces in the Z -field strength ($\sqrt{\frac{1}{2} Z_{\mu\nu} Z^{\mu\nu}}$) and in the scalar field modulus.

After the rescaling (4), it becomes clear that the only free parameters in our model are β ($\beta \equiv m_H^2/m_z^2 = 8\lambda/g_z^2$) and θ_W . It is well known that with $\theta_W = \pi/2$ and $\beta < 1$ we have semilocal strings that are stable [4], and numerical simulations show segment formation and linkage [5]. Moreover, for $\sin^2\theta_W \lesssim 1$, $\beta < 1$, there is a regime, albeit a rather narrow one, where infinitely long strings are perturbatively stable [7,10]. Bearing these results in mind, the parameter space investigated in our simulations was $0.9 \leq \sin^2\theta_W \leq 1$ and $0.05 \leq \beta \leq 1.5$.

Simulation and visualization were performed on 64^3 , 128^3 and 256^3 lattices using the Cray T3E at NERSC, and high-performance computing facilities at University of Sussex and University of Groningen. Our quoted results all come from 256^3 simulations.

IV. RESULTS

To test our code, we began by reproducing known results for cosmic and semilocal string networks, and for infinitely long, axially-symmetric Z -strings (made possible by our periodic boundary conditions as long as strings are simulated in pairs to keep the net flux equal to zero) in both the stable and unstable regimes, in particular verifying that the Z -strings disappeared in the unstable regime.

Having checked the code, we then ran it for values of the two free parameters (θ_W, β) throughout the regime of interest, using the same initial conditions for each parameter pair. We chose to carry out one large simulation at each point in parameter space rather than many smaller ones, which gives improved dynamical range. As expected, after an initial transient, the typical configuration observed is a dumbbell — a segment of electroweak string joining a monopole/antimonopole pair. By continuity, for parameter values sufficiently close to the stable semilocal case we expect the monopole interactions to lead to the joining of strings to form longer segments.

The simulations show that some short segments of Z -string do join as expected. The joining rate is, however, lower than in the semilocal case, and decreases both as $\sin^2\theta_W$ is decreased and as β is increased. Thus, some segments which would eventually join in the semilocal case are seen instead to collapse in the electroweak case due to string tension. This is not surprising: in the semilocal case, we have global monopoles at the string ends, which have divergent scalar gradient energy and are more efficient at finding neighbouring monopoles. In the electroweak case, the monopoles at the string ends are proper magnetic monopoles, and the scalar gradients are cancelled much more efficiently by gauge fields. As $\sin^2\theta_W \rightarrow 1$ the cores become larger, and eventually overlap, making segments join. But as we move away from the semilocal case, the cores become smaller and the joining becomes less important.

Fig. 1 shows timeslices of two typical simulations, with the different colours corresponding to the A - and Z -field strengths.¹ The Z -field has a string-like form, whereas the A -field at the string ends is a spherical shell, corresponding to spherical magnetic monopoles. The A -field morphology can also be tube-like, denoting interaction between monopoles, illustrating the complexity of the overall dynamics. The interplay between string tension and monopole–antimonopole attraction causes some strings to shrink until they disappear, and others join to form longer strings.

To compare the number of defects in the semilocal and electroweak cases, we plot the number of lattice sites with Z -magnetic field strength ($\sqrt{\frac{1}{2}Z_{\mu\nu}Z^{\mu\nu}}$) greater than 25% of the maximum field strength found in the NO case (see Fig. 2). The number of lattice sites, and hence length of string, decreases more rapidly in the electroweak case as either $\sin^2\theta_W$ decreases or β grows.

At early times the configurations in different simulations are very similar. During the symmetry-breaking transient (the very first time steps) no defects exist. As the scalar field takes on a non-zero value a large number of very small string segments emerge, then the magnetic monopoles become visible at the ends of the segments due to the gathering of A -magnetic flux there. The upper panels of Fig. 1 show the Z - and A -magnetic field strength of two different simulations at time $t = 50$.

As the system evolves, we see that in only one of the simulations do the small segments grow and connect to their neighbours, allowing the defect network to persist. In the lower panels the configuration at time $t = 200$ can be seen. In one case there are long strings and connections are still happening, whereas in the other almost all of the dumbbells have annihilated. In particular, in the first case the final configuration contains strings which are much longer at the end of the simulation than any present in the early stages.

We wish to determine the parameter space for which the string network persists. The stability of the corresponding infinite Z -strings is a necessary condition for persistence, but not sufficient since the physically realizable collection

¹Further colour images and movies can be found at www.nersc.gov/~borrill/defects/electroweak.html

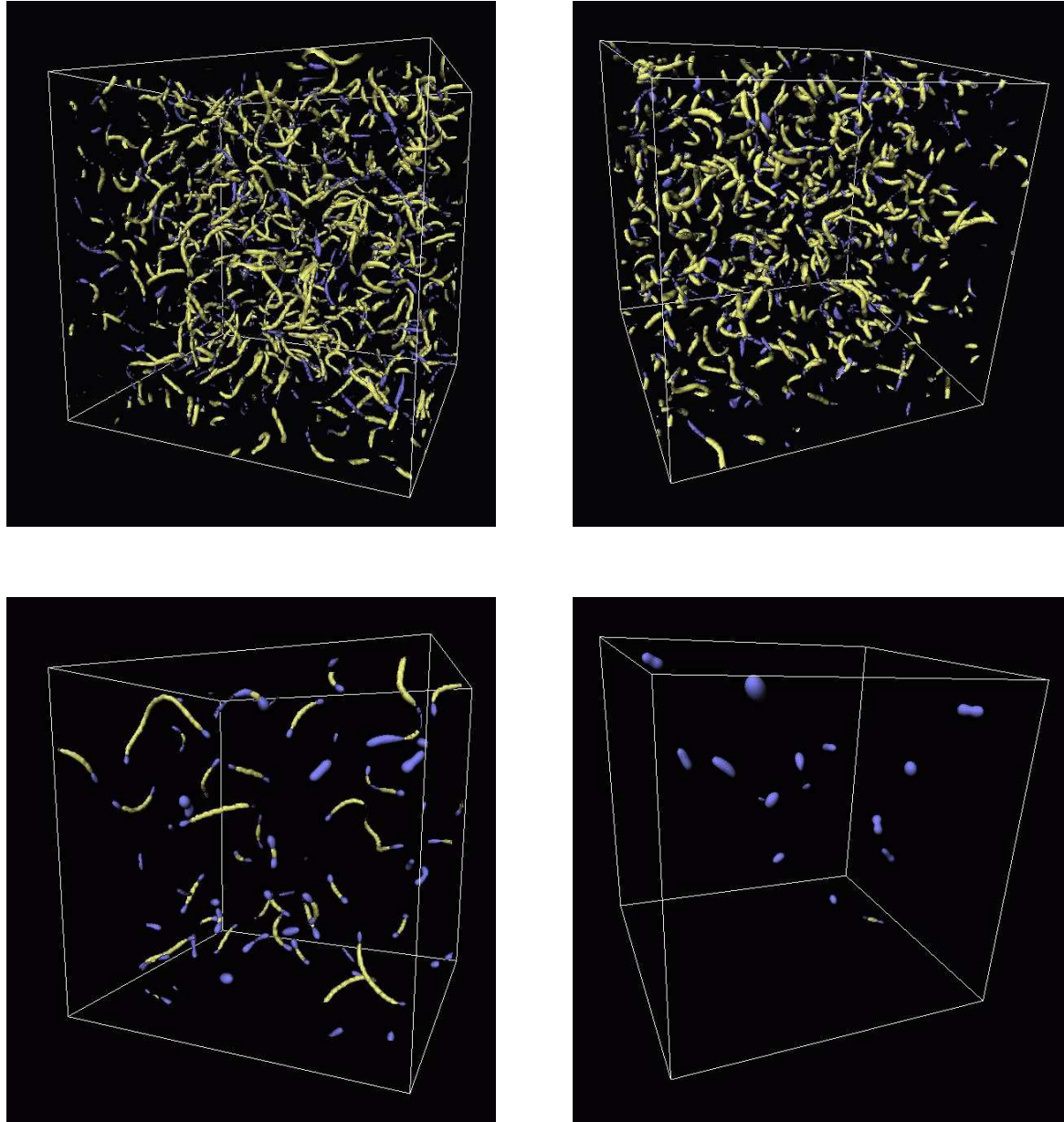


FIG. 1. Isosurfaces of the Z - and A -magnetic field strengths for two different simulations, shown as the light and dark colour respectively. The left panels show $\beta = 0.1$, $\sin^2 \theta_W = 0.994$ (persistent regime) and the right ones $\beta = 0.5$, $\sin^2 \theta_W = 0.995$ (non-persistent regime). The top row is at an early stage of the simulation $t = 50$, while the lower is at the end $t = 200$. Note that in the first case there remain some long strings at the end of the simulation and connection can still occur. In the second all the defects are about to disappear.

of finite initial string segments may not link up. We therefore expect the persistence region of parameter space to lie entirely within the stability region.

To estimate the persistence of Z -strings we need to define a criterion to decide when defects are lasting long enough. There is clearly some degree of arbitrariness in how this criterion is set, and we have been guided by inspecting visually the evolution in different parameter regimes. In order to construct the persistence region in parameter space we simulated the system in 256^3 boxes with periodic boundary conditions, and considered persistence to have occurred if at time $t = 200$ there are more than 1000 lattice sites with a Z -magnetic flux greater than 25% of the maximum of the NO simulation for the same β . For example, for $\beta = 0.3$, we can see in Fig. 2 that persistence defined this way is exhibited only for $\sin^2 \theta_W > 0.995$. From a suite of simulations using this criterion we obtain the ‘persistence limit’ shown in Fig. 3. As anticipated, the persistence region covers only a subset of the stability region, with persistence only

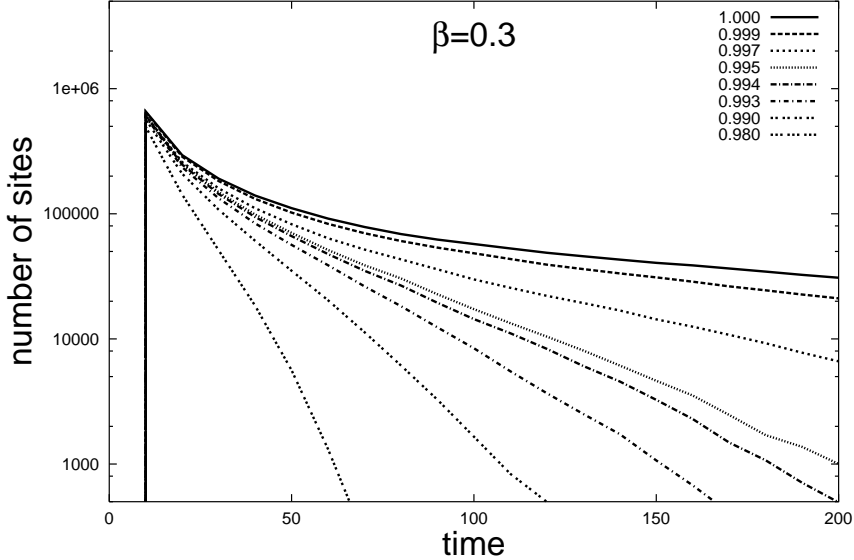


FIG. 2. The number of lattice points with Z -field strength ($\sqrt{\frac{1}{2}Z_{\mu\nu}Z^{\mu\nu}}$) bigger than 25% of the maximum value in the NO case, calculated in a series of 256^3 simulations, for $\beta = 0.3$. The different lines correspond to different choices of the weak mixing angle θ_W (values shown are for $\sin^2\theta_W$). Note that in our criterion for persistence (see text), for the chosen β , the defects are considered to live long enough for $\sin^2\theta_W \gtrsim 0.995$. Using different initial conditions for the simulations give similar behaviour.

for values of $\sin^2\theta_W$ extremely close to one. Another possible criterion for persistence which can be easily automated is the presence at late times of strings that are reasonably long compared to their width.² At time $t = 200$, the condition that there be strings at least five times their width leads to the second persistence line drawn in Fig. 3.

Since the actual version of electroweak theory in our Universe lies well outside the stability zone, it will not exhibit a persistent network, though it remains possible that a similar phase transition might take place at a higher energy, leading to persistent defects which could survive to the present.

V. CONCLUSIONS

The numerical simulations described here show that a significant non-topological defect network can form in the electroweak phase transition. The dynamics of such a network are extremely complicated, driven by string segment linkings and by isolated strings shrinking, and the details are highly sensitive to the two model parameters θ_W and β . Our principal result is that in some regions of parameter space a persistent network of defects can form, with the possibility that they might survive to the present epoch (though the actual version of electroweak theory in our Universe lies outside this parameter regime). This confirms and extends similar results obtained in the semilocal case [5].

The result might seem to be in disagreement with previous work of Nagasawa and Yokoyama [13], but this is not the case since here we are considering the time evolution of a network and not just the initial configuration; the generation of the string segments is intrinsically dynamical and cannot be studied using initial condition arguments. In fact, the first timesteps in such simulations correspond more to a numerical transient, in which physically reasonable initial conditions are established, than an actual phase transition. Only after this initial transient can the evolution of the network be trusted, and this is what determines whether the defects persist or decay. Given the primary role played

²To automate the calculation of the length of the individual strings, we compute the volume of each segment of string by counting the number of connected points whose Z -magnetic field is at least 25% of the maximum in a NO string at the same value of β . Then, the volume is divided by the cross-sectional area of the NO string. Finally, to obtain the length-to-width ratio, we divide it by the width of the corresponding NO string, using as “width” twice the distance between the center of the NO string and the point where the field strength is 25% of the maximum.

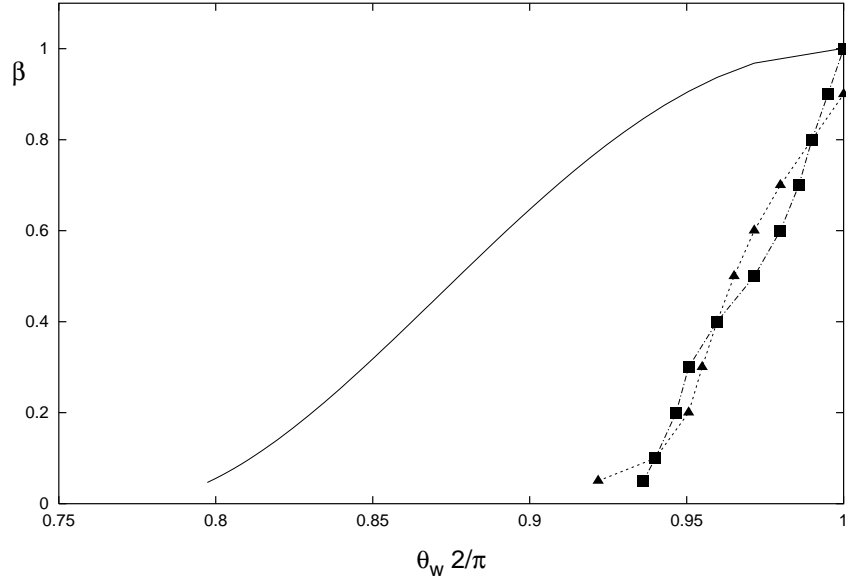


FIG. 3. The solid line is the semi-analytical curve marking the stability transition for infinite, axially-symmetric Z -strings [10], and the points mark the edge of the persistence region obtained in our simulations, using both criteria described in the text. As expected, the persistence limit lies entirely within the stability zone. The squares are obtained considering that the defects are persistent if at $t = 200$ there are more than 1000 points with a magnetic field strength higher than 25% of the maximum (see text); the triangles are obtained by considering persistent those defects which at $t = 200$ are at least 5 times longer than their width.

by the gauge fields, it would be interesting to know if our conclusions generalize to non-topological string defects in other models such as the two-Higgs standard model [14,15].

ACKNOWLEDGMENTS

AA and JU acknowledge support from grants CICYT AEN99-0315 and UPV 063.310-EB187/98. JU is also partially supported by a Marie Curie Fellowship of the European Community programme HUMAN POTENTIAL under contract number HPMT-CT-2000-00096. This research used resources of the National Energy Research Scientific Computing Center, which is supported by the Office of Science of the U.S. Department of Energy under Contract No. DE-AC03-76SF00098. JU is grateful to the Lawrence Berkeley National Laboratory at the University of California, the Kapteyn Institute and the Institute for Theoretical Physics at the University of Groningen, and the Astronomy Centre at the University of Sussex for their hospitality during visits, and the use of their computer facilities including those of the Sussex High-Performance Computing Initiative. We thank Mark Hindmarsh for useful discussions.

- [1] T. W. B. Kibble, J. Phys. **A9**, 1387 (1976).
- [2] A. Vilenkin and E.P.S. Shellard, *Cosmic Strings and Other Topological Defects*, Cambridge University Press, Cambridge, 1994.
- [3] T. Vachaspati and A. Achúcarro, Phys. Rev. D **44**, 3067 (1991).
- [4] M. Hindmarsh, Phys. Rev. Lett. **68**, 1263 (1992).
- [5] A. Achúcarro, J. Borrill and A. R. Liddle, Phys. Rev. Lett. **82**, 3742 (1999).
- [6] Y. Nambu, Nucl. Phys. **B130**, 505 (1977).
- [7] T. Vachaspati, Phys. Rev. Lett. **68**, 1977 (1992); **69** 216(E) (1992).
- [8] A. Achúcarro and T. Vachaspati, Phys. Rep. **327**, 347 (2000).
- [9] H. B. Nielsen and P. Olesen, Nucl. Phys. **B61**, 45 (1973).
- [10] M. James, L. Perivolaropoulos and T. Vachaspati, Nucl. Phys. **B395**, 534 (1993).

- [11] M. Hindmarsh, in: J. C. Romão, F. Freire (eds), Proceedings of the NATO Workshop on “Electroweak Physics and the Early Universe”, Sintra, Portugal, 1994; Series B: Physics Vol. 338, Plenum Press, New York, 1994.
- [12] A. Achúcarro, J. Borrill and A. R. Liddle, Phys. Rev. D **57**, 3742 (1998).
- [13] M. Nagasawa and J. Yokoyama, Phys. Rev. Lett. **77**, 2166 (1996).
- [14] M. A. Earnshaw, M. James, Phys. Rev. **D48** 5818 (1993).
- [15] C. Bachas, B. Rai and T. N. Tomaras, Phys. Rev. Lett **82**, 2443 (1999).